Light mass galileon and late time acceleration of the Universe

R. Myrzakulov[1*], M. Shahalam[2†]
[1] *Department of General and Theoretical Physics, Eurasian National University, Astana, Kazakhstan*
[2] *Center For Theoretical Physics, Jamia Millia Islamia, New Delhi, India*
(Dated: June 30, 2015)

We study Galileon scalar field model by considering the lowest order Galileon term in the lagrangian , $(\partial_\mu\phi)^2\Box\phi$ by invoking a field potential. We use Statefinder hierarchy to distinguish the light mass galileon models with different potentials amongst themselves and from the ΛCDM behaviour. The Om diagnostic is applied to cosmological dynamics and observational constraints on the model parameters are studied using SN+Hubble+BAO data.

arXiv:1407.7798v3 [gr-qc] 27 Jun 2015

I. INTRODUCTION

The late time cosmic acceleration is supported by the cosmological observations directly [1] and indirectly [2, 3]. Dark energy might be responsible for driving the cosmic acceleration of Universe [4]. Cosmological constant is one of the simplest candidate of dark energy however it is plagued by the serious problems such as fine tuning and cosmic coincidence [5]. To understand the nature of dark energy, this is important to understand whether it is cosmological constant or it has dynamics. The scalar field models of dark energy [6] were introduced to give a dynamical solution to the cosmological constant problem.

Recently a class of dynamical dark energy models based on the large scale modification of gravity have been proposed to describe the late time acceleration of Universe and Galileon gravity is one of them. The action of Galileon field (in absence of potential) is invariant under Galilean shift symmetry $\phi(x) \to \phi(x) + b_\mu x^\mu + c$ in the Minkowski background, where b_μ and c are the constant four vector and scalar respectively. Nicolis *et al.* [7] considered five field Lagrangians $\mathcal{L}_i$ $(i = 1, \cdots, 5)$ in four dimensional flat space time. $\mathcal{L}_1$ is linear, $\mathcal{L}_2$ represents the standard kinetic term, $\mathcal{L}_3 = (\partial_\mu\phi)^2\Box\phi$ is the Vainshtein term which has three galileon fields, and this term is associated to the decoupling limit of Dvali, Gabadadze, and Porrati (DGP) model [8]. $\mathcal{L}_4$ and $\mathcal{L}_5$ accommodate higher order non linear derivative terms with four and five $\phi's$ respectively. Cosmological dynamics in flat FRW Universe with these terms has been investigated in reference [9].

At least one of the higher order Galileon Lagrangian is needed to obtain a stable de sitter solution [10]. In this paper we focus on $\mathcal{L}_3$ but add a general potential term to galileon field. We use Statefinder hierarchy to differentiate the light mass galileon models with different potentials amongst themselves and from the ΛCDM behaviour. The Om diagnostic is applied to cosmological dynamics and observational constraints on the model parameters are studied using SN+Hubble+BAO data jointly. The paper is organized as follows. The equations of motion of light mass galileon are presented in section II. In section III, the statefinder hierarchy and late time cosmological evolution is studied. The Om diagnostic is discussed in section IV. We investigate the constraints on the model parameters by applying latest observational data in section V.

II. EQUATIONS OF MOTION

Let us consider the action for Galileon field keeping upto the third order term in the lagrangian with a field potential $V(\phi)$ in the action.

$$S = \int d^4x\sqrt{-g}\Big[\frac{M_{\rm pl}^2}{2}R - \frac{1}{2}(\nabla\phi)^2\Big(1 + \frac{\beta}{M^3}\Box\phi\Big) - V(\phi)\Big] + \mathcal{S}_m. \tag{1}$$

Here, $M_{\rm pl}^2 = 1/8\pi G$ is the reduced Planck mass. β is a dimensionless constant. $\mathcal{S}_m$ designates matter action. M is a constant of mass dimension one; we fix $M = M_{\rm pl}$.

* E-mail address: rmyrzakulov@gmail.com
† E-mail address: mohdshahamu@gmail.com

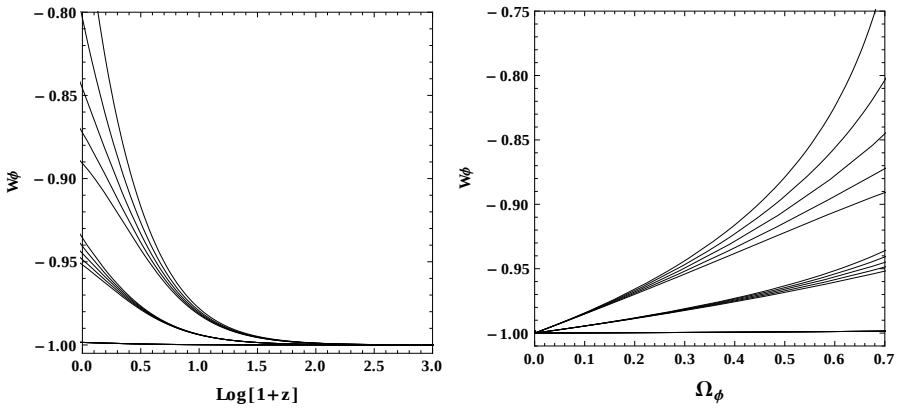

FIG. 1: This figure shows the evolution of w_ϕ versus the redshift z and Ω_ϕ. There are three sets for $\lambda_i = 0.1, 0.6, 1$ from bottom to top and $V(\phi) \sim \phi, \phi^2, e^\phi, \phi^{-2}, \phi^{-1}$ from top to bottom in every set.

In a homogenous isotropic flat FRW Universe, the equations of motion are obtained by varying the action (eq (1)) with respect to metric tensor $g_{\mu\nu}$ and scalar field ϕ,

$$3M_{\rm pl}^2 H^2 = \rho_m + \frac{\dot\phi^2}{2}\Big(1 - 6\frac{\beta}{M_{\rm pl}^3}H\dot\phi\Big) + V(\phi)\,, \tag{2}$$

$$M_{pl}^2(2\dot H + 3H^2) = -\frac{\dot\phi^2}{2}\Big(1 + 2\frac{\beta}{M_{\rm pl}^3}\ddot\phi\Big) + V(\phi), \tag{3}$$

$$3H\dot\phi + \ddot\phi - 3\frac{\beta}{M_{\rm pl}^3}\dot\phi\Big(3H^2\dot\phi + \dot H\dot\phi + 2H\ddot\phi\Big) + V'(\phi) = 0, \tag{4}$$

The above equations are augmented by the matter conservation equation,

$$\dot\rho_m + 3H\rho_m = 0. \tag{5}$$

We introduce the following dimensionless quantities

$$x = \frac{\dot\phi}{\sqrt{6}HM_{\rm pl}}\,, \quad y = \frac{\sqrt{V}}{\sqrt{3}HM_{\rm pl}} \tag{6}$$

$$\epsilon = -6\frac{\beta}{M_{\rm pl}^3}H\dot\phi\,, \quad \lambda = -M_{\rm pl}\frac{V'}{V} \tag{7}$$

to form an autonomous system of evolution equations:

$$x' = x\Big(\frac{\ddot\phi}{H\dot\phi} - \frac{\dot H}{H^2}\Big), \tag{8}$$

$$y' = -y\Big(\sqrt{\frac{3}{2}}\lambda x + \frac{\dot H}{H^2}\Big), \tag{9}$$

$$\epsilon' = \epsilon\Big(\frac{\ddot\phi}{H\dot\phi} + \frac{\dot H}{H^2}\Big), \tag{10}$$

$$\lambda' = \sqrt{6}x\lambda^2(1-\Gamma), \tag{11}$$

where prime ($'$) denotes derivative with respect to $\ln a$, $\Gamma = \frac{VV_{,\phi\phi}}{V_{,\phi}^2}$ and

$$\frac{\dot H}{H^2} = \frac{2(1+\epsilon)(-3+3y^2) - 3x^2(2+4\epsilon+\epsilon^2) + \sqrt{6}x\epsilon y^2\lambda}{4+4\epsilon+x^2\epsilon^2}, \tag{12}$$

$$\frac{\ddot\phi}{H\dot\phi} = \frac{3x^3\epsilon - x\Big(12+\epsilon(3+3y^2)\Big) + 2\sqrt{6}y^2\lambda}{x(4+4\epsilon+x^2\epsilon^2)}, \tag{13}$$

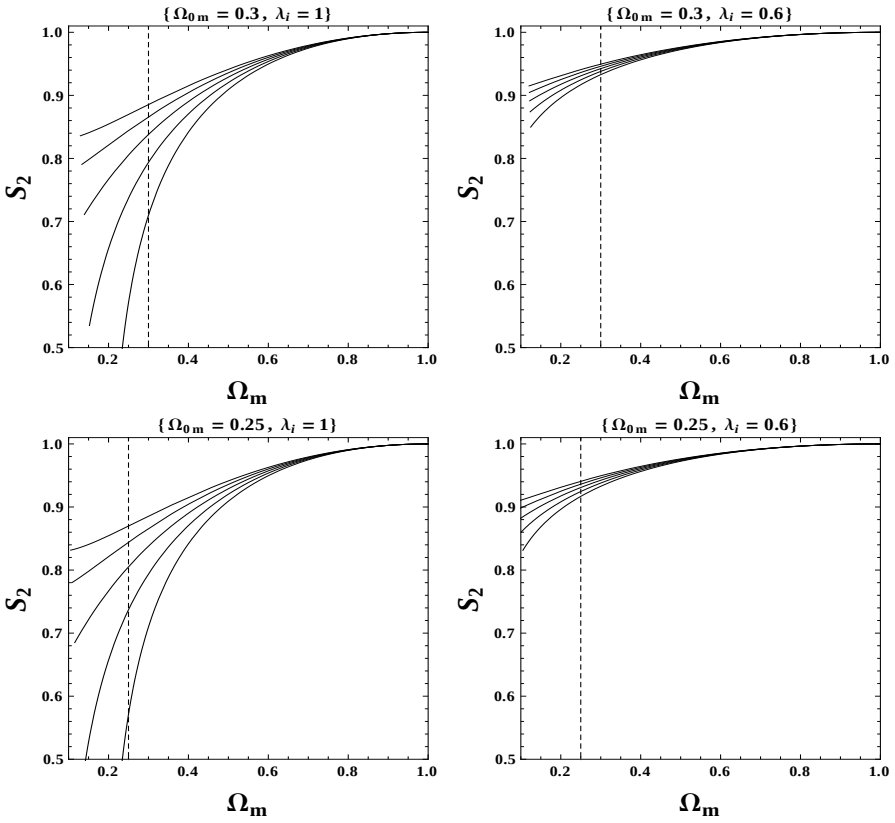

FIG. 2: This figure shows the evolution of S_2 versus Ω_m for different potentials $V(\phi) \sim \phi, \phi^2, e^{\phi}, \phi^{-2}, \phi^{-1}$ from bottom to top and for different values of λ_i and Ω_{0m}. The vertical dashed line shows the present epoch (z = 0).

The equation of state for the field ϕ is given as,

$$w_{eff} = -1 - \frac{2\dot{H}}{3H^2}, \tag{14}$$

$$w_{\phi} = \frac{w_{eff} - w_m \Omega_m}{1 - \Omega_m}, \tag{15}$$

where $w_m = 0$ for standard dust matter. We evolve the system from $z \approx 1000$ (decoupling era) till any redshift we wish. We assume the ϕ field was frozen initially due to large hubble damping. This is alike to the thawing class of models [11]. We choose different potentials for which $\Gamma = \frac{VV_{,\phi\phi}}{V_{,\phi}^2}$= constant.

III. THE STATEFINDER HIERARCHY AND LATE TIME COSMOLOGICAL EVOLUTION

Consider the Taylor expansion of the scale factor around the present era ($t = t_0$) as:

$$\frac{a(t)}{a(t_0)} = 1 + \sum_{n=1}^{\infty} \frac{\alpha_n(t_0)}{n!} \left[H_0(t - t_0)\right]^n, \tag{16}$$

where,

$$\alpha_n = \frac{d^n a}{dt^n}/(aH^n), \tag{17}$$

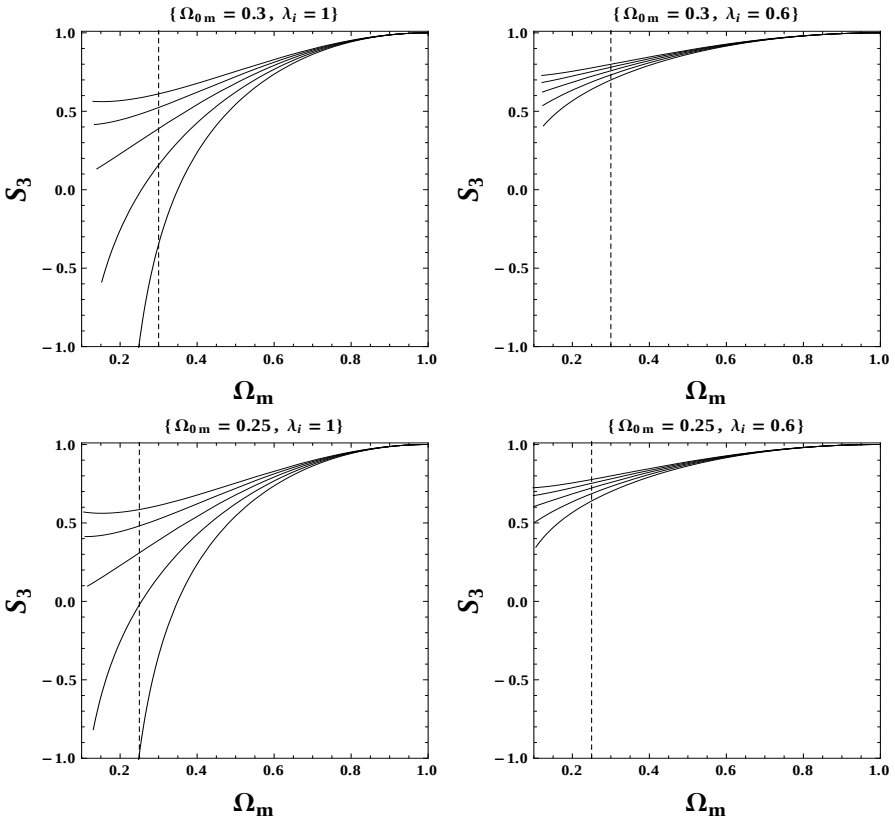

FIG. 3: Same as figure 2 but for S_3.

It is easy to see that $-\alpha_2 = q$ is the deceleration parameter; α_3 and α_4 is associated to the Statefinder r and Snap s respectively and so on. These parameters in terms of hubble parameter can be written as,

$$\alpha_2 = \frac{\ddot{a}}{aH^2} \equiv \frac{\dot{H}}{H^2} + 1 \tag{18}$$

$$\alpha_3 = \frac{\dddot{a}}{aH^3} \equiv \frac{\ddot{H}}{H^3} + 3\frac{\dot{H}}{H^2} + 1 \tag{19}$$

$$\alpha_4 = \frac{\ddddot{a}}{aH^4} \equiv 1 + \frac{\dddot{H}}{H^4} + 4\frac{\ddot{H}}{H^3} + 3\frac{\dot{H}^2}{H^4} + 6\frac{\dot{H}}{H^2} \quad \text{and so on} \tag{20}$$

Using equations (16) and (17) Arabsalmani *et al.* [12] define Statefinder hierarchy as:

$$S_2 := \alpha_2 + \frac{3}{2}\Omega_m, \tag{21}$$

$$S_3 := \alpha_3, \tag{22}$$

$$S_4 := \alpha_4 + \frac{3^2}{2}\Omega_m, \tag{23}$$

$$S_5 := \alpha_5 - 3\Omega_m - \frac{3^3}{2}\Omega_m^2, \tag{24}$$

$$S_6 := \alpha_6 + \frac{3^3}{2}\Omega_m + 3^4\Omega_m^2 + \frac{3^4}{4}\Omega_m^3 \quad \text{and so on} \tag{25}$$

where $\Omega_m = \Omega_{0\mathrm{m}}(1+z)^3/h^2(z)$. It is notable to see that for ΛCDM, $S_n = 1$ during the entire course of cosmic expansion. Now we use various combinations of S_n, to study the evolution of light mass galileon model with different potentials.

The initial value of λ i.e λ_i is an important parameter. It tells about the departure from the ΛCDM behaviour. Figure 1 shows that for smaller values of λ_i ($\lambda_i = 0.1$) the models with different potentials can rarely be distinguished amongst themselves and from ΛCDM (w = -1). As λ_i grows, all the models with different potentials start deviating from each other as well as from ΛCDM (w = -1). Furthermore, as we

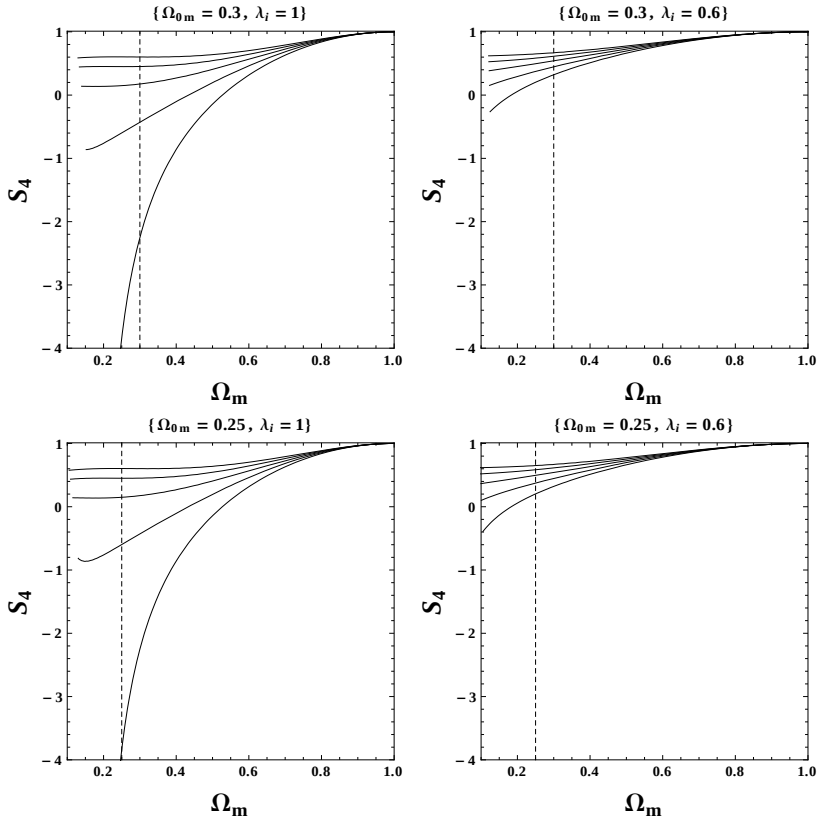

FIG. 4: Same as figure 2 but for S_4.

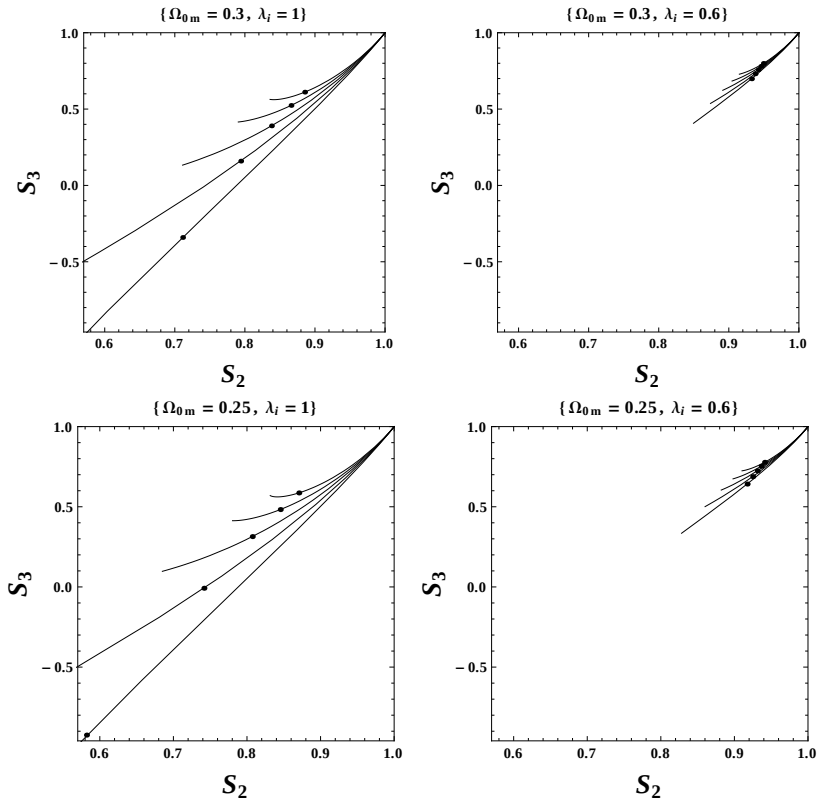

FIG. 5: This figure shows the evolution of S_3 versus S_2 for different potentials $V(\phi) \sim \phi, \phi^2, e^{\phi}, \phi^{-2}, \phi^{-1}$ from bottom to top and for different values of λ_i and Ω_{0m}. The black dots show the present epoch (z = 0).

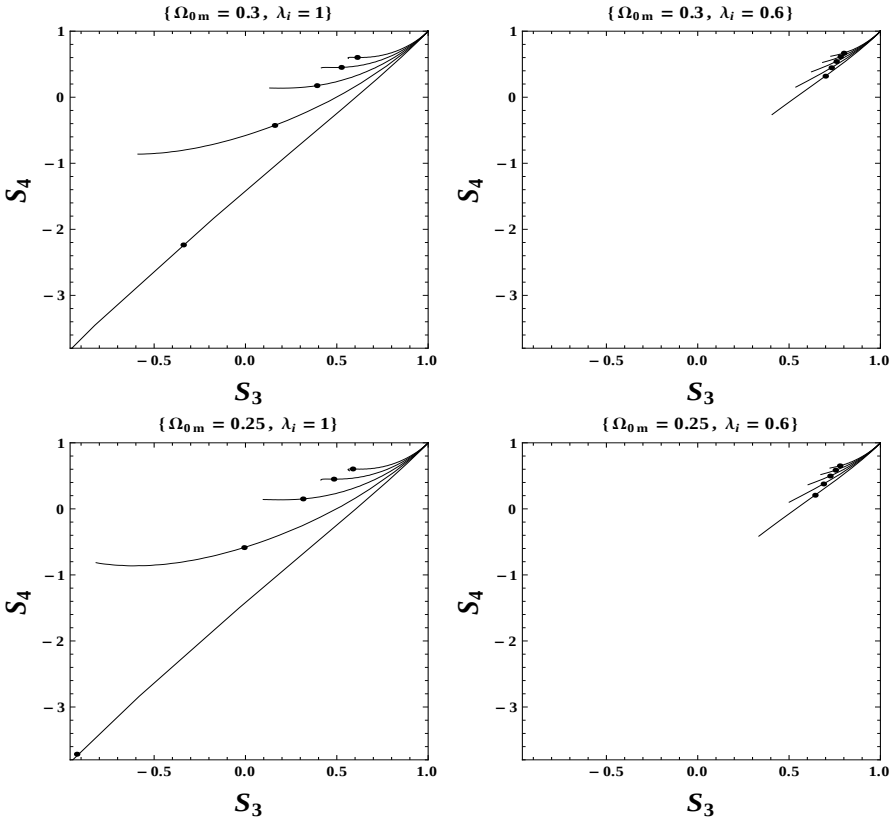

FIG. 6: Same as figure 5 but for S_4 versus S_3.

go for higher λ_i, the equation of state w_ϕ for linear potential has the largest departure from ΛCDM. In figure 2, we show the evolution of different potentials for different values of λ_i and Ω_{0m} in $S_2 - \Omega_m$ plane. As we have shown in the case of equation of state, here also the departure from the ΛCDM is small and large for smaller and larger values of λ_i respectively. The linear potential shows the highest deviation from ΛCDM for $\lambda_i = 1$. The models with various potentials nearly degenerate for smaller values of λ_i whereas for higher values of λ_i the models are showing non degeneracy. Moreover, departure from the ΛCDM as well as among different potentials are larger for smaller values of Ω_{0m}.

In figure 3, we show the evolution of models with different potentials for different values of λ_i and Ω_{0m} in $S_3 - \Omega_m$ plane. The departure from the ΛCDM as well as among different potentials are higher for smaller values of Ω_{0m}. For smaller and larger values of λ_i the models with different potentials nearly degenerate and non degenerate respectively. Next, we show the evolution of different potentials in the $S_4 - \Omega_m$ plane in figure 4. Here too, the models with various potentials depart more for smaller Ω_{0m} and larger λ_i. In figures 5 and 6 we show the evolution of different potentials in the $S_3 - S_2$ and $S_4 - S_3$ plane respectively. In these figures also the models with various potentials depart more for smaller and larger values of Ω_{0m} and λ_i respectively.

IV. Om DIAGNOSTIC

The Om, a geometrical diagnostic, is constructed from the hubble parameter and depends upon the first derivative of scale factor. It discriminates different dynamical dark energy models from ΛCDM with correct and incorrect values of the matter density. For ΛCDM model, Om has same values at different redshifts. This implies that non-evolving nature of Om provides a null test for cosmological constant . The Om for spatially flat Universe is defined as [13]:

$$Om(x) \equiv \frac{H^2(x)/H_0^2 - 1}{x^3 - 1}, \quad x = 1 + z \ . \tag{26}$$

The hubble parameter for constant equation of state is defined as,

$$H^2(x) = H_0^2(\Omega_{0m}x^3 + (1 - \Omega_{0m})x^{3(1+w)}), \tag{27}$$

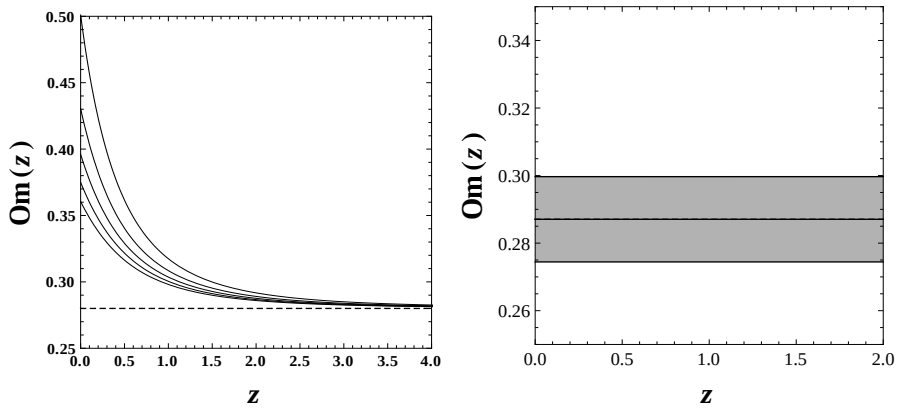

FIG. 7: This figure shows the evolution of Om versus z. Left plot shows the Om behaviour for the models with different potentials $V(\phi) \sim \phi, \phi^2, e^{\phi}, \phi^{-2}, \phi^{-1}$ from top to bottom with $\lambda_i = 1$ and $\Omega_{0m} = 0.28$. Right plot shows the Om behaviour for the model with linear potential. The solid line shows the best fitted behaviour inside 1σ confidance level. It looks same as ΛCDM due to the very small best fit value of $\lambda_i \approx 0.002505$. Here we use $\Omega_{0m} = 0.287057$.

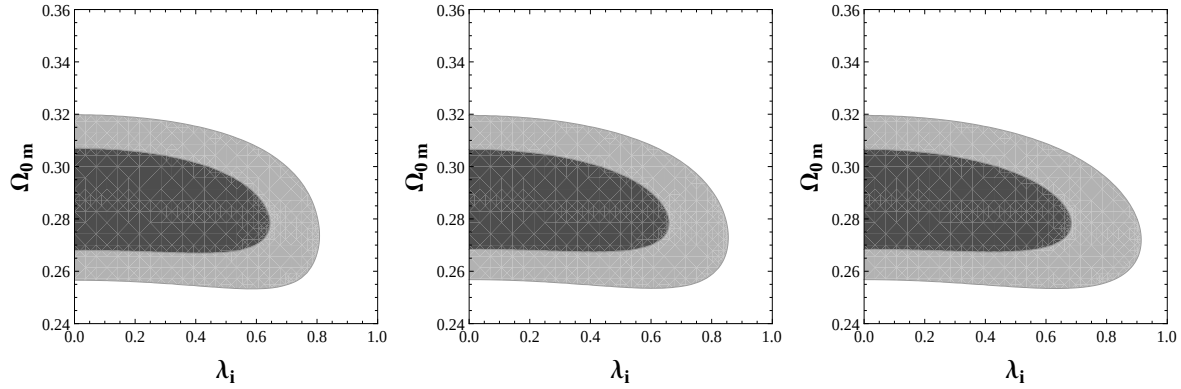

FIG. 8: This figure shows the 1σ (dark shaded) and 2σ (light shaded) likelihood contours in the $\lambda_i - \Omega_{0m}$ plane. Left, middle and right plots are for linear, quadratic and exponential potentials respectively.

Therefore,

$$Om(x) = \Omega_{0m} + (1 - \Omega_{0m})\frac{x^{3(1+w)} - 1}{x^3 - 1} \ , \tag{28}$$

from equation (28) we conclude that,

For ΛCDM ($w = -1$), $Om(x) = \Omega_{0m}$, This implies that Om has zero curvature. For quintessence ($w > -1$), $Om(x) < \Omega_{0m}$, This implies that Om has negative curvature. For phantom ($w < -1$), $Om(x) > \Omega_{0m}$, This implies that Om has positive curvature.

We, therefore, conclude that $Om(x) = \Omega_{0m}$ *iff* dark energy is a cosmological constant. It is interesting to see that Om provides a null test of the ΛCDM hypothesis. In this section we want to show that Om has negative curvature for quintessence dark energy models. The Om behaviour for the models with different potentials is shown in the left plot of figure 7, where Om has negative curvature. In the right plot of figure 7 we show the best fitted behaviour inside 1σ confidence level for the linear potential. The best fitted behaviour is constant and same as ΛCDM because the best fit value of the parameter $\lambda_i \approx 0.002505$ is very small. The best fitted behaviour of the models with other potentials is same as ΛCDM due to the smaller best fit value of λ_i. This type of behaviour for equation of state is shown in figure 1 where for small values of λ_i equation of state is nearly same as in case of ΛCDM.

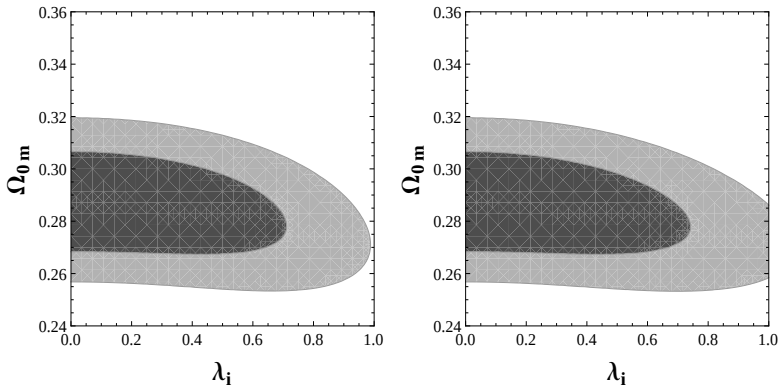

FIG. 9: Same as figure 8 but left one is for inverse square potential while right one is for inverse potential.

TABLE I: $H(z)$ measurements (in units $[\mathrm{km\,s^{-1}Mpc^{-1}}]$) and their errors [15].

z	$H(z)$	σ_H	Reference
0.070	69	19.6	[17]
0.100	69	12	[18]
0.120	68.6	26.2	[17]
0.170	83	8	[18]
0.179	75	4	[19]
0.199	75	5	[19]
0.200	72.9	29.6	[17]
0.270	77	14	[18]
0.280	88.8	36.6	[17]
0.350	76.3	5.6	[20]
0.352	83	14	[19]
0.400	95	17	[18]
0.440	82.6	7.8	[21]
0.480	97	62	[22]
0.593	104	13	[19]
0.600	87.9	6.1	[21]
0.680	92	8	[19]
0.730	97.3	7.0	[21]
0.781	105	12	[19]
0.875	125	17	[19]
0.880	90	40	[22]
0.900	117	23	[18]
1.037	154	20	[19]
1.300	168	17	[18]
1.430	177	18	[18]
1.530	140	14	[18]
1.750	202	40	[18]
2.300	224	8	[23]

V. OBSERVATIONAL CONSTRAINTS

We put observational constraints on the model parameters λ_i and Ω_{0m} by applying latest observational data. We consider the supernova Type Ia observation which is one of the direct probes of the cosmic expansion. We use latest Union2.1 data compilation [14] consisting of 580 data points.

The observable quantity μ is the distance modulus which is defined as, $\mu = m - M = 5\log D_L + \mu_0$, where m and M are the apparent and absolute magnitudes of the supernovae, μ_0 is a nuisance parameter which is marginalized and D_L is the luminosity distance defined as $D_L(z) = (1+z)\int_0^z \frac{dz'}{H(z')/H_0}$.

Next, we use latest 28 observational data points of hubble parameter at different redshifts compiled by Farroq et. al [15]. We take H_0 from Planck 2013 results [16] to complete the data set. The values are shown in Table I.

TABLE II: Values of $\frac{d_A(z_\star)}{D_V(Z_{BAO})}$ for different values of z_{BAO}.

z_{BAO}	0.106	0.2	0.35	0.44	0.6	0.73
$\frac{d_A(z_\star)}{D_V(Z_{BAO})}$	30.95 ± 1.46	17.55 ± 0.60	10.11 ± 0.37	8.44 ± 0.67	6.69 ± 0.33	5.45 ± 0.31

TABLE III: Best fit values of the model parameters for different potentials.

Potentials	λ_i	Ω_{0m}
$V(\phi) \propto \phi$	0.002505	0.287057
$V(\phi) \propto \phi^2$	0.002165	do
$V(\phi) \propto e^{\phi}$	0.001884	do
$V(\phi) \propto \phi^{-2}$	0.003233	do
$V(\phi) \propto \phi^{-1}$	0.002964	do

finally, we use BAO data of $\frac{d_A(z_\star)}{D_V(Z_{BAO})}$ [24–29], where $d_A(z) = \int_0^z \frac{dz'}{H(z')}$ is the co-moving angular-diameter distance, $D_V(z) = \left(d_A(z)^2 \frac{z}{H(z)}\right)^{\frac{1}{3}}$ is the dilation scale and $z_\star \approx 1091$ is the decoupling time. Data required for this analysis is shown in Table II.

The $\chi^2_{\rm BAO}$ is described in reference [29] and defined as,

$$\chi^2_{\rm BAO} = X^t C^{-1} X\,, \tag{29}$$

where,

$$X = \begin{pmatrix} \frac{d_A(z_\star)}{D_V(0.106)} - 30.95 \\ \frac{d_A(z_\star)}{D_V(0.2)} - 17.55 \\ \frac{d_A(z_\star)}{D_V(0.35)} - 10.11 \\ \frac{d_A(z_\star)}{D_V(0.44)} - 8.44 \\ \frac{d_A(z_\star)}{D_V(0.6)} - 6.69 \\ \frac{d_A(z_\star)}{D_V(0.73)} - 5.45 \end{pmatrix}, \tag{30}$$

and the inverse covariance matrix,

$$C^{-1} = \begin{pmatrix} 0.48435 & -0.101383 & -0.164945 & -0.0305703 & -0.097874 & -0.106738 \\ -0.101383 & 3.2882 & -2.45497 & -0.0787898 & -0.252254 & -0.2751 \\ -0.164945 & -2.45499 & 9.55916 & -0.128187 & -0.410404 & -0.447574 \\ -0.0305703 & -0.0787898 & -0.128187 & 2.78728 & -2.75632 & 1.16437 \\ -0.097874 & -0.252254 & -0.410404 & -2.75632 & 14.9245 & -7.32441 \\ -0.106738 & -0.2751 & -0.447574 & 1.16437 & -7.32441 & 14.5022 \end{pmatrix}. \tag{31}$$

The results are shown in figures 8 and 9 where we show 1σ (dark shaded) and 2σ (light shaded) likelihood contours in the $\lambda_i - \Omega_{0m}$ plane. The right plot of figure 9 shows that inverse potential has highest allowed deviation from the ΛCDM behaviour. The best fit values of the model parameters are shown in Table III.

VI. CONCLUSIONS

In this paper, we restrict ourselves to the lowest order galileon lagrangian $\mathcal{L}_3$ but add a general potential term $V(\phi)$ to the Lagrangian and explore the late time cosmological evolution of light mass galileon with different choices for $V(\phi)$. We acquire that the ϕ field is initially frozen due to large hubble friction and acts as a cosmological constant. We do not acquire slow roll conditions for the potentials under consideration thereby λ_i is a free parameter in the model. The deviation from $w = -1$ (ΛCDM) depends upon the value of λ_i. For smaller values of λ_i, the departure is small and all potentials behave like cosmological constant throughout. As the value of λ_i grows, the evolution begins departing from $w = -1$ (ΛCDM). By applying statefinder hierarchy, we discuss degeneracies for the various potentials. It is found that S_3 is best suited for removing the degeneracy amongst the models we considered in case of $\Omega_{0m} \simeq 0.25, \lambda_i \simeq 1$. However, the same lies out side 1σ bound. We should admit that shift symmetry in the Minkowski background breaks by adding a potential. However, since the mass of galileon is of the order of H_0, the effect of symmetry breaking is mild.

We also use Om diagnostic to show that Om has negative slope for the models having equation of state $w > -1$, and this is shown in the left plot of figure 7 for $\lambda_i = 1$. The right plot of figure 7 shows that Om acts like a cosmological constant due to the small best fit value of the parameter λ_i. We used SN+Hubble+BAO data to constraint the model parameters.

Acknowledgement

We thank M. Sami for his useful comments and suggestions. MS thanks to Sumit Kumar and M. W. Hossain for fruitful discussions.

[1] A. G. Riess et al., Astron. J. **116**, 1009 (1998); S. Perlmutter et al., Astrophys. J. **517**, 565 (1999); J. L. Tonry et al., Astrophys. J. **594**, 1 (2003).

[2] A. Melchiorri et al., Astrophys. J. Lett. **536**, L63 (2000); A. E. Lange et al., Phys. Rev. D **63**, 042001 (2001); A. H. Jaffe et al., Phys. Rev. Lett. **86**, 3475 (2001); C. B. Netterfield et al., Astrophys. J. **571**, 604 (2002); N. W. Halverson et al., Astrophys. J. **568**, 38 (2002).

[3] S. Bridle, O. Lahab, J. P. Ostriker and P. J. Steinhardt, Science **299**, 1532 (2003); C. Bennett et al., Astrophys. J. Suppl. Ser. **148**, 1 (2003); G. Hinshaw et al., Astrophys. J. Suppl. Ser. **148**, 135 (2003); A. Kogut et al., Astrophys. J. Suppl. Ser. **148**, 161 (2003); D. N. Spergel et al., Astrophys. J. Suppl. Ser. **148**, 175 (2003).

[4] E. J. Copeland, M. Sami and S. Tsujikawa, Int. J. Mod. Phys. D **15**, 1753 (2006); Miao Li, Xiao-Dong Li, Shuang Wang, arXiv:1103.5870

[5] S. Weinberg, Rev. Mod. Phys. **61**, 1 (1989);
V. Sahni and A. A. Starobinsky, Int. J. Mod. Phys. D **9**, 373 (2000) [astro-ph/9904398];
S. M. Carroll, Living Rev. Rel. **4**, 1 (2001) [astro-ph/0004075];
P. J. E. Peebles and B. Ratra, Rev. Mod. Phys. **75**, 559 (2003) [astro-ph/0207347];
T. Padmanabhan, Phys. Rept. **380**, 235 (2003) [hep-th/0212290]

[6] P. J. E. Peebles and B. Ratra, apj **325**, L17 (1988); C. Wetterich, Nucl. Phys. B **302**, 668 (1988); M. S. Turner and M. White, Phys. Rev. D **56**, 4439 (1997); R. R. Caldwell, R. Dave and P. J. Steinhardt, Phys. Rev. Lett. **80**, 1582 (1998); I. Zlatev, L. M. Wang and P. J. Steinhardt, Phys. Rev. Lett. **82**, 896 (1999).

[7] A. Nicolis, R. Rattazzi and E. Trincherini, Phys. Rev. D, **79**, 064036 (2009).

[8] G. R. Dvali, G. Gabaddze and M. Porrati, Phys. Lett. B, **485**, 208, (2000). M. A. Luty, M. Porrati and R. Rattazzi, JHEP, **09**, 029 (2003); A. Nicolis and R. Rattazzi, JHEP, **06**, 059 (2004).

[9] A. De Felice and S. Tsujikawa, Cosmology of a covariant Galileon field, Phys. Rev. Lett. 105 (2010) 111301 [arXiv:1007.2700] [INSPIRE]; S. Appleby and E.V. Linder, The Paths of Gravity in Galileon Cosmology, JCAP 03 (2012) 043 [arXiv:1112.1981] [INSPIRE]; M. Jamil, D. Momeni and R. Myrzakulov, "Observational constraints on non-minimally coupled Galileon model," Eur. Phys. J. C **73** (2013) 2347 [arXiv:1302.0129 [physics.gen-ph]]; E.V. Linder, The Direction of Gravity, arXiv:1201.5127 [INSPIRE]; A. De Felice and S. Tsujikawa, Cosmological constraints on extended Galileon models, JCAP 03 (2012) 025 [arXiv:1112.1774] [INSPIRE]; C. Burrage, C. de Rham and L. Heisenberg, de Sitter Galileon, JCAP 05 (2011) 025 [arXiv:1104.0155] [INSPIRE]; A. De Felice, R. Kase and S. Tsujikawa, Matter perturbations in Galileon cosmology, Phys. Rev. D 83 (2011) 043515 [arXiv:1011.6132] [INSPIRE]; S. Nesseris, A. De Felice and S. Tsujikawa, Observational constraints on Galileon cosmology, Phys. Rev. D 82 (2010) 124054 [arXiv:1010.0407] [INSPIRE]; C. Burrage, C. de Rham, D. Seery and A.J. Tolley, Galileon inflation, JCAP 01 (2011) 014 [arXiv:1009.2497] [INSPIRE]; A. De Felice and S. Tsujikawa, Generalized Galileon cosmology, Phys. Rev. D 84 (2011) 124029 [arXiv:1008.4236] [INSPIRE]; A. Ali, R. Gannouji, M.W. Hossain and M. Sami, Light mass galileons: Cosmo-

logical dynamics, mass screening and observational constraints, Phys. Lett. B 718 (2012) 5 [arXiv:1207.3959], M. W. Hossain, Anjan A. Sen, Do Observations favour Galileon Over Quintessence?Phys. Lett. B., **713**, 140, (2012) [arXiv:1201.6192], M. Sami, M. Shahalam, M. Skugoreva, A. Toporensky, Phys. Rev. D **86**, 103532 (2012) [arXiv:1207.6691], R. Myrzakulov and M. Shahalam, JCAP 10 (2013) 047 [arXiv:1303.0194], Sampurnanand and A. A. Sen, DBI Galileon and late acceleration of the universe, JCAP 12 (2012) 019 [arXiv:1208.0179], G. Leon and E. N. Saridakis, JCAP **1303**, 025 (2013) [arXiv:1211.3088 [astro-ph.CO]].

[10] A. Ali, R. Gannouji and M. Sami, Modified gravity a la Galileon: Late time cosmic acceleration and observational constraints, Phys. Rev. D 82 (2010) 103015 [arXiv:1008.1588] [INSPIRE]; R. Gannouji and M. Sami, Galileon gravity and its relevance to late time cosmic acceleration, Phys. Rev. D 82 (2010) 024011 [arXiv:1004.2808] [INSPIRE];

[11] R. J. Scherrer and A. .A. Sen, Phys. Rev. D, **77**, 083515 (2008); R. J. Scherrer and A. .A. Sen, Phys. Rev. D, **78**, 067303 (2008); S. Sen, A. A. Sen and M. Sami, Phys. Lett. B., **686**, 1, (2010); S. del Campo, C. R. Fadragas, R. Herrera, C. Leiva, G. Leon and J. Saavedra, Phys. Rev. D **88**, 023532 (2013) [arXiv:1303.5779 [astro-ph.CO]]; D. Escobar, C. R. Fadragas, G. Leon and Y. Leyva, Astrophys. Space Sci. **349**, 575 (2014) [arXiv:1301.2570 [gr-qc]].

[12] M. Arabsalmani, V. Sahni,The Statefinder hierarchy: An extended null diagnostic for concordance cosmology, Phys. Rev. D **83**, 043501 (2011).

[13] V. Sahni, A. Shafieloo and A. A. Starobinsky, Two new diagnostics of dark energy, Phys. Rev. D **78**, 103502 (2008). A. Shafieloo, V. Sahni and A. A. Starobinsky, New null diagnostic customized for reconstructing the properties of dark energy from baryon acoustic oscillations data, Phys. Rev. D **86**, 103527 (2012).

[14] N. Suzuki, D. Rubin, C. Lidman, G. Aldering, R. Amanullah, K. Barbary, L. F. Barrientos and J. Botyanszki *et al.*, Astrophys. J. **746**, 85 (2012) [arXiv:1105.3470 [astro-ph.CO]].

[15] O. Farooq and B. Ratra, Astrophys. J. **766**, L7 (2013) [arXiv:1301.5243 [astro-ph.CO]].

[16] P. A. R. Ade *et al.* [Planck Collaboration], arXiv:1303.5076 [astro-ph.CO].

[17] C. Zhang, H. Zhang, S. Yuan, T. -J. Zhang and Y. -C. Sun, arXiv:1207.4541 [astro-ph.CO].

[18] J. Simon, L. Verde and R. Jimenez, Phys. Rev. D **71**, 123001 (2005) [astro-ph/0412269].

[19] M. Moresco, L. Verde, L. Pozzetti, R. Jimenez and A. Cimatti, JCAP **1207**, 053 (2012) [arXiv:1201.6658 [astro-ph.CO]].

[20] C. -H. Chuang and Y. Wang, arXiv:1209.0210 [astro-ph.CO].

[21] C. Blake, S. Brough, M. Colless, C. Contreras, W. Couch, S. Croom, D. Croton and T. Davis *et al.*, Mon. Not. Roy. Astron. Soc. **425**, 405 (2012) [arXiv:1204.3674 [astro-ph.CO]].

[22] D. Stern, R. Jimenez, L. Verde, M. Kamionkowski and S. A. Stanford, JCAP **1002**, 008 (2010) [arXiv:0907.3149 [astro-ph.CO]].

[23] N. G. Busca, T. Delubac, J. Rich, S. Bailey, A. Font-Ribera, D. Kirkby, J. M. Le Goff and M. M. Pieri *et al.*, Astron. Astrophys. **552**, A96 (2013) [arXiv:1211.2616 [astro-ph.CO]].

[24] C. Blake, E. Kazin, F. Beutler, T. Davis, D. Parkinson, S. Brough, M. Colless and C. Contreras *et al.*, Mon. Not. Roy. Astron. Soc. **418**, 1707 (2011) [arXiv:1108.2635 [astro-ph.CO]].

[25] W. J. Percival *et al.* [SDSS Collaboration], Mon. Not. Roy. Astron. Soc. **401**, 2148 (2010) [arXiv:0907.1660 [astro-ph.CO]].

[26] F. Beutler, C. Blake, M. Colless, D. H. Jones, L. Staveley-Smith, L. Campbell, Q. Parker and W. Saunders *et al.*, Mon. Not. Roy. Astron. Soc. **416**, 3017 (2011) [arXiv:1106.3366 [astro-ph.CO]].

[27] N. Jarosik, C. L. Bennett, J. Dunkley, B. Gold, M. R. Greason, M. Halpern, R. S. Hill and G. Hinshaw *et al.*, Astrophys. J. Suppl. **192**, 14 (2011) [arXiv:1001.4744 [astro-ph.CO]].

[28] D. J. Eisenstein *et al.* [SDSS Collaboration], Astrophys. J. **633**, 560 (2005) [astro-ph/0501171].

[29] R. Giostri, M. V. d. Santos, I. Waga, R. R. R. Reis, M. O. Calvao and B. L. Lago, JCAP **1203**, 027 (2012) [arXiv:1203.3213 [astro-ph.CO]].